

Title: A hands-on tutorial on a modelling framework for projections of climate change impacts on health.

Authors: Ana M. Vicedo-Cabrera<sup>a</sup>, Francesco Sera<sup>a</sup>, Antonio Gasparri<sup>a,b</sup>.

- a. Department of Public Health, Environments and Society, London School of Hygiene and Tropical Medicine, London, United Kingdom.
- b. Centre for Statistical Methodology, London School of Hygiene and Tropical Medicine, London, United Kingdom

Corresponding author:

Ana M. Vicedo-Cabrera, PhD

Department of Public Health, Environments and Society, London School of Hygiene and Tropical Medicine.

15-17 Tavistock Place, London WC1H 9SH. United Kingdom

ana.vicedo-cabrera@lshtm.ac.uk

Running title: A tutorial on health impact projections

Conflicts of interest: none.

Sources of funding: This work was primarily supported by the Medical Research Council-UK [MR/M022625/1].

As Supplementary Digital Content, we provide the data and R code that illustrates the analytical steps described in this contribution and reproduces the figures shown in the main manuscript.

1 **Abstract**

2 Reliable estimates of future health impacts due to climate change are needed to inform  
3 and contribute to the design of efficient adaptation and mitigation strategies. However,  
4 projecting health burdens associated to specific environmental stressors is a challenging  
5 task, due to the complex risk patterns and inherent uncertainty of future climate  
6 scenarios. These assessments involve multi-disciplinary knowledge, requiring expertise  
7 in epidemiology, statistics, and climate science, among other subjects. Here, we present  
8 a methodological framework to estimate future health impacts under climate change  
9 scenarios based on a defined set of assumptions and advanced statistical techniques  
10 developed in time-series analysis in environmental epidemiology. The proposed  
11 methodology is illustrated through a step-by-step hands-on tutorial structured in well-  
12 defined sections that cover the main methodological steps and essential elements. Each  
13 section provides a thorough description of each step, along with a discussion on  
14 available analytical options and the rationale on the choices made in the proposed  
15 framework. The illustration is complemented with a practical example of study using real-  
16 world data and a series of R scripts included as Supplementary Digital Content, which  
17 facilitates its replication and extension on other environmental stressors, outcomes,  
18 study settings, and projection scenarios. Users should critically assess the potential  
19 modelling alternatives and modify the framework and R code to adapt them to their  
20 research on health impact projections.

21  
22  
23  
24  
25  
26  
27  
28  
29  
30  
31  
32

## 33 **Background**

34 Climate change is one of the most important environmental challenges that humanity will  
35 face in the coming decades. Quantifying future health burdens associated to global  
36 warming is therefore a major priority for the scientific community, as attested by the  
37 increasing number of publications on health impact projections. Several studies have  
38 focused on direct impacts of environmental stressors, such as non-optimal temperature  
39 and air pollution.<sup>1-5</sup> Generally, these projection studies follow a common methodological  
40 scheme. The basic idea consists in applying risk functions on simulated future exposure  
41 distributions generated by climate change models under specific emissions scenarios.  
42 However, this scheme entails important methodological challenges due, for instance, to  
43 the complex patterns of health risks associated with environmental stressors, the  
44 inherent uncertainty of potential future climate change processes, and the set of (rarely  
45 stated) assumptions.<sup>6</sup> A wide variety of data sources, statistical approaches and  
46 assumptions have been applied so far, as summarized and discussed in previous  
47 reviews.<sup>6-8</sup> However, a structured illustration that covers the important steps and discuss  
48 the most recent statistical developments is still lacking.

49 Here, we illustrate a methodological framework to estimate health impact projections  
50 under climate change scenarios, built on clearly defined assumptions and state-of-the-  
51 art statistical methodologies developed in time-series analysis in environmental  
52 epidemiology. This contribution extends a methodology previously presented to project  
53 temperature-related excess mortality in climate change scenarios.<sup>5,9</sup> The proposed  
54 framework is illustrated through a hands-on tutorial, structured in well-differentiated steps  
55 that cover each of the methodological issues and the essential elements. Each section  
56 provides a detailed description of the methodology and a discussion on the potential  
57 assumptions and limitations, compared to other available choices. The text is  
58 complemented with a practical illustration of a projection study using real-world data, and  
59 a series of R scripts included as Supplementary Digital Content, with updated versions  
60 available in the personal website and GitHub repository of the last author. The  
61 methodological framework and R code can be modified and adapted to a broad range of  
62 health impact projection studies, optionally assessing different environmental stressors  
63 and health outcomes, and with different study settings.

64

## 65 **Illustrative example**

66 The practical example consists of a projection study on temperature-related mortality  
67 impacts in the city of London, United Kingdom. The dataset includes observed daily

68 mean temperature and total number of deaths in London between 1990 and 2012. This  
69 is part of the large database collected within the Multi-City Multi-Country (MCC) network  
70 (<http://mccstudy.lshhtm.ac.uk/>), and has been previously used as example in other  
71 manuscripts.<sup>10</sup> We complement these observed data with daily-modelled temperature  
72 series for historical (1950-2005) and future (2006-2100) periods, projected under  
73 scenarios defined within the Coupled Model Intercomparison Project Phase 5 of  
74 Intergovernmental Panel on Climate Change (IPCC).<sup>11</sup> Climate data was obtained,  
75 processed and made available by the Inter-Sectoral Impact Model Intercomparison  
76 Project (ISI-MIP, <https://www.isimip.org/>).<sup>12</sup> Further details on the modelled data is  
77 provided in the Section 2 of the tutorial.

78

## 79 **Tutorial on the modelling framework**

### 80 1. Estimation of exposure-response associations

81 One critical step in health impact projection studies is to appropriately define the  
82 relationship between the exposure to the environmental stressor of interest and the  
83 health outcome. While this information can be based on association estimates reported  
84 in the literature,<sup>13,14</sup> this often requires strong assumptions due to extrapolation across  
85 geographical areas, and simplification of usually complex relationships.

86 A more appropriate approach is to directly estimate the relationship using actual  
87 epidemiological data, for which several statistical methods are available.<sup>15,16</sup> Among  
88 these, time series analysis using aggregated data has been shown to be ideal to assess  
89 short-term associations in environmental epidemiology,<sup>17</sup> and often applied in climate  
90 change projection studies.<sup>1,18,19</sup>

91 A representation of the standard time series regression model is provided by the  
92 following equation:

$$93 \quad \log[E(Y_t)] = \alpha + f(x_t; \boldsymbol{\theta}) + s(t; \boldsymbol{\beta}) + \sum_{p=1}^P h_p(z_{pt}; \boldsymbol{\gamma}_p) \quad (1)$$

94 where typically the outcome  $Y_t$  corresponds to daily counts assumed to follow a Poisson  
95 distribution with overdispersion, the function  $f(x_t; \boldsymbol{\theta})$  specifies the association with the  
96 environmental exposure of interest  $x$  at time  $t$ ,  $s(t; \boldsymbol{\beta})$  represents the baseline trend  
97 which captures the effect of confounders changing slowly over time (i.e., seasonal and  
98 long-term trends), and  $h_p(z_{pt}; \boldsymbol{\gamma}_p)$  models the contribution of other confounders varying  
99 on a daily basis.

100 The exposure-response association can be modelled using different types of function  $f$ ,  
101 ranging from simple indicators for extreme exposure events, to linear or linear-threshold

102 shapes, to distributed lag non-linear models (DLNMs) representing complex exposure-  
103 lag-response surfaces.<sup>20</sup> The selection of the function depends on the environmental  
104 stressor, for instance measured as a continuous exposure (e.g., temperature, rain fall)  
105 or defined extreme event (e.g., heat wave, floods), and the assumed dependency with  
106 the health outcome. As shown below, wrong assumptions on the shape of the  
107 dependency can introduce important biases in estimates and projections.

108 In our example, the environmental stressor and the outcome corresponds to historical  
109 series of daily mean temperature and death counts ( $T_{obs}$  and  $D_{obs}$ ). Our main choice for  
110 the exposure-response function  $f(x_t)$  is represented by a DLNM through a bi-  
111 dimensional cross-basis term, using flexible natural cubic spline functions to model both  
112 exposure-response and lagged-response dimensions, accounting for 21 days of lag,  
113 following previous work.<sup>10</sup> As further described in Section 4 of this tutorial, the choice of  
114 natural splines allows the log-linear extrapolation of the function beyond the boundaries  
115 of the observed series, a step needed to project the risk using the modelled temperature.  
116 Figure 1A shows the resulting 3-D plot of the estimated exposure-lag-response  
117 association, and Figure 1B represents the overall cumulative exposure-response  
118 association across up to 21 days of lag. As expected, we observe a non-linear  
119 temperature-mortality relationship, with increases in relative risk (RR) above and below  
120 the minimum mortality temperature ( $T_{mm}$ ) that correspond to heat and cold associations,  
121 respectively. At the same time, risks are distributed differently across time, with  
122 immediate heat-mortality and more delayed cold-mortality associations (Figure 1A).

123 Alternative models with different specifications of the exposure-response association,  
124 such as linear or double-threshold parameterizations, are shown in Figure 1C. While  
125 simpler, however these choices seem less ideal for modelling the mortality risk of non-  
126 optimal temperature, highlighting the importance of the selection of suitable functions to  
127 represent the association of interest, and the potential bias of inappropriate  
128 simplifications.

129

## 130 2. Projected temperature and mortality series

131 Two additional essential elements needed in health impact projection studies are the  
132 information on future climatic and population scenarios.

133 Data on future distribution of the environmental stressor (e.g., temperature, precipitation,  
134 air pollution levels) are commonly based on specific scenarios that account for changes  
135 in multiple and often inter-related factors. For instance, socioeconomic and technological  
136 changes, population growth and land use changes can affect pathways of greenhouse

137 gases emissions or atmospheric concentrations of other pollutants, which in turn will  
138 determine trends in global warming and potential levels of specific environmental  
139 exposures.<sup>21</sup> Under each scenario, these trends can be generated from general  
140 circulation models (GCMs), which offer projections of future conditions based on specific  
141 and simplified assumptions.<sup>21</sup> To have a better representation of future trends, the usual  
142 approach is to combine impact estimates obtained either using more than one model per  
143 scenario or using ensemble members output from multiple runs of the same climate  
144 model, but with different initial conditions.<sup>6,7</sup>

145 In our worked example, we applied the first approach by including modelled temperature  
146 data from 5 different GCMs for two climate change scenarios, defined as representative  
147 concentration pathways 4.5 and 8.5 (RCP4.5 and RCP8.5).<sup>22,23</sup> Figure 2 shows the  
148 temporal trends in temperature for the historical (1971-2005) and future (2006-2100)  
149 periods projected in London under the two scenarios, depicted as GCM-ensemble  
150 averages (solid lines) and associated variability (shaded areas). As discussed later in  
151 Section 6, the availability of exposure trends from multiple models can be used to  
152 determine the related uncertainty of the projected health impacts.

153 Projection exercises also depend on representations of future mortality trends,  
154 determined by the demographic structure and outcome baseline rates. Data on these  
155 population scenarios can be built following different approaches based on the adopted  
156 assumptions. The simplest procedure consists in assuming that populations and  
157 outcome rates will remain constant in the future, thus isolating the climate effect from  
158 other important trends.<sup>24-26</sup> However, other studies relied on population projections  
159 derived from predictive models under varying levels of future fertility, mortality and  
160 migration,<sup>27-29</sup> a procedure that requires additional assumptions.

161 In our example, we illustrate an application of the former method. First, we compute an  
162 annual series of total mortality counts as the average for each day of the year from  
163 observed daily deaths, thus keeping into account the seasonal structure of the observed  
164 mortality series (Figure 3). The annual series is then replicated along the whole  
165 projection period. The extension to more complex scenarios requires the derivation of  
166 age-specific mortality series, obtained using projection methods that model changes in  
167 the demographic structure and baseline rates, as further explained in Section 7 of this  
168 tutorial.

169

170 3. Downscaling and calibration

171 Climate simulations of historical periods usually show systematic deviations from the  
172 real-world observations. This can be explained by real differences due to the different  
173 geographical resolution of the data (gridded versus point-source), or to biases due to  
174 poor performance of climate models, occurring in areas with sparse information from  
175 meteorological stations. These deviations should be carefully considered in climate  
176 change projection studies, as the predicted impacts will depend on the alignment of  
177 observed and modelled series.<sup>30,31</sup> Corrections of biases related to these two aspects  
178 have been defined separately as downscaling and calibration, although in most cases  
179 they rely on similar analytic procedures. Downscaling refers to the process of obtaining  
180 location-specific climate information from global or regional models that provide data at  
181 a larger geographical resolution, and is based on either dynamical or statistical methods.<sup>7</sup>  
182 Conversely, calibration is a more general concept of re-aligning two series of data, in this  
183 case observed and modelled series.

184 Bias correction methods have been proposed for both statistical downscaling and  
185 calibration, and encompass various different techniques with varying degree of  
186 complexity, ranging from basic statistical approaches (i.e., use of additive or  
187 multiplicative corrections, shifted distribution), to more complex statistical procedures.<sup>31</sup>  
188 However, limited evidence exists about the potential impact of the choice of method on  
189 the estimated projections.

190 In the present tutorial, the model outputs from the GCMs are firstly downscaled through  
191 bi-linear interpolation at a  $0.5^\circ \times 0.5^\circ$  spatial resolution and linear interpolated by day of  
192 the year. The resulting series are then calibrated with the observed data using the bias-  
193 correction method developed within ISI-MIP.<sup>32</sup> This ensures that the trend and variability  
194 of the original data are preserved by adjusting the cumulative distribution of the simulated  
195 data to the observed one. In detail, the monthly variability and mean are corrected only  
196 using a constant offset or multiplicative correction factor that corrects for long-term  
197 differences between the simulated and observed monthly mean data in the historical  
198 period.<sup>32</sup> Figure 4 shows a comparison between the modelled series from a specific GCM  
199 ( $T_{mod}$ , green area and line), and the observed series ( $T_{obs}$ , black area and line), in terms  
200 of their overall and cumulative distribution (left and right panels, respectively). It can be  
201 noted that the modelled series is shifted towards colder ranges, likely for the reasons  
202 mentioned above. As discussed, this would create a bias in the future projections. The  
203 bias-correction procedure described above calibrates the modelled series ( $T_{mod}^*$ , green  
204 dashed line), re-aligning it to the observed one (Figure 4, right panel).

205

206 4. Extrapolation of exposure-response curves

207 Risk estimates obtained over historical periods do not automatically apply to future  
208 scenarios, due to several reasons. For instance, it is possible that the estimated  
209 exposure-response association will be different in the future, due to for example  
210 adaptation or changes in vulnerability of the population. However, even when assuming  
211 no changes in risk, the future distribution of a specific environmental stressor is likely to  
212 be different to that observed in the present days, and can extend further than the region  
213 of the estimated exposure-response curve. Thus, we need to perform an additional step  
214 consisting in the extrapolation of the exposure-response beyond the observed  
215 boundaries. This, however, implies the adoption of additional assumptions on the  
216 hypothetical shape of the association over the unobserved range.

217 As shown in Figure 5 (top panel), a viable method is based on a log-linear extrapolation  
218 of the curve beyond the observed boundaries. The use of a natural cubic spline function  
219 to model the exposure-response dimension ensures this non-linear extrapolation,  
220 although this step can be more problematic when applying different functions.  
221 Nonetheless, this entails a series of strong assumptions on the future risk associated to  
222 environmental factors. The first assumption, mentioned above, is that the exposure-  
223 response association estimated on the currently observed range will not change in the  
224 future, for instance as a result of changes in susceptibility of the population, as discussed  
225 in Section 7. The second assumption is that the extrapolation represents appropriately  
226 the risk over the unobserved range. In addition, due to the nature of the epidemiological  
227 approaches, the extrapolation of the curve over un-observed ranges constitutes an  
228 important source of uncertainty to our projection estimates. This last issue will be further  
229 described in Section 6.

230

231 5. Projection and quantification of the impact

232 The next step of the proposed analytical framework consists in estimating the projected  
233 health impacts estimates by applying the exposure-response association estimates over  
234 the modelled series of the specific environmental stressor and outcome. Previous studies  
235 reported measures of impact using various measures, for instance in terms of percent  
236 changes in the rate of the outcome, excess mortality or morbidity, or attributable  
237 fractions.<sup>5,18,33</sup> Our framework incorporates the procedure previously developed to  
238 estimate the impacts in terms of attributable fractions within in time series analysis,  
239 applicable either with the DLNM framework or with simpler exposure-response  
240 dependencies.<sup>34</sup>



241 In brief, the method consists in computing for each day of the series the number of cases  
 242 attributed to a specific environmental stressor based on the estimated risk and the level  
 243 of exposure in that specific day. Then daily attributable numbers are aggregated by  
 244 defined intervals of time in the future period. It can be also expressed in terms of  
 245 attributable fraction computed as the ratio with the corresponding total number of cases.  
 246 Finally, projection studies are mostly interested in obtaining comparative measures of  
 247 impact between climate change scenarios or timeframes, which can be easily computed  
 248 as differences in attributable numbers or fractions.

249 In the specific setting of the example of study, we estimate the attributable number of  
 250 deaths  $D_{attr}$  due to non-optimal temperatures using the calibrated temperature series  
 251  $T_{mod}^*$  following:

$$252 \quad D_{attr} = D \cdot \left( 1 - e^{-\left( f^*(T_{mod}^*; \theta_b^*) - s^*(T_{mm}; \theta_b^*) \right)} \right) \quad (2)$$

253

254 where  $f^*$  and  $\theta^*$  represents the uni-dimensional overall cumulative exposure-response  
 255 curves with reduced lag dimension, derived from the bi-dimensional term estimated in  
 256 Section 1 of the tutorial. In Eq.2, we can also separate components due to heat and cold  
 257 by summing the subsets corresponding to days with temperatures higher or lower than  
 258  $T_{mm}$ .<sup>10</sup> The same computation can be used with simpler exposure-response functions,  
 259 and the equation simplifies to the usual (RR-1)/RR in the case of linear or binary  
 260 unlagged relationships.

261 The selection of the  $T_{mm}$  is a critical step in the quantification of the attributable mortality.  
 262 While this step has been shown to have little impact in well-powered multi-location  
 263 studies relying on best linear unbiased predictions, this choice can be problematic in  
 264 single-location analyses that can be affected by highly imprecise exposure-response  
 265 curves.<sup>10,35</sup>

266 Figure 5 (mid and bottom panels) shows the distributions of temperatures and estimated  
 267 attributable mortality, respectively, for the historic and future period in London under the  
 268 assumption of stable populations and no changes in vulnerability. We can observe that  
 269 the mortality burden due to cold temperatures is currently much larger than for heat,  
 270 especially across the moderate cold temperatures. However, if we compare the  
 271 estimates between each of the two periods, we can see that heat-attributable mortality  
 272 will substantially increase in the future by 4.0% (95% empirical confidence interval (eCI):  
 273 0.7-6.8), while mortality due to cold will be reduced by 3.3% (95% eCI: 4.3-1.9). A  
 274 description on the computation of the eCI is provided in the following section. The same

275 methodological procedure can be applied to derive attributable mortality for more  
276 complex scenarios, as illustrated in Section 7.

277

## 278 6. Ensemble estimates and quantification of uncertainty

279 A key methodological issue in projection studies is to properly identify and deal with the  
280 different sources of uncertainty involved in the projection of impacts in future scenarios.  
281 These include those related to purely statistical aspects, such as the imprecision of the  
282 estimated exposure-response function, and the inherent uncertainty of the exposure  
283 simulations obtained from the climate and circulation models.<sup>6</sup>

284 Based on the proposed framework, uncertainty arises mainly from two main sources: the  
285 estimation of the exposure-response function, especially regarding the range over which  
286 we extrapolated the curve, and climate projections. These are represented by the  
287 covariance matrix  $V(\theta_b)$  of the model coefficients estimated in Equation 1 defining the  
288 exposure-response function, and the variability of the modelled series generated in each  
289 GCM (Figure 2), respectively. In the tutorial, we quantify this uncertainty by generating  
290 1000 samples of the coefficients through Monte Carlo simulations, assuming a  
291 multivariate normal distribution for the estimated spline model coefficients, and then  
292 generating results for each of the five GCMs.<sup>34</sup> We report the results as point estimates,  
293 using the average across climate models (GCM-ensemble) obtained by the estimated  
294 coefficients, and as eCI, defined as the 2.5<sup>th</sup> and 97.5<sup>th</sup> percentiles of the empirical  
295 distribution of the attributable mortality across coefficients samples and GCMs. These  
296 eCIs account for both sources of uncertainty.

297 As briefly mentioned before, we did not account for additional uncertainty derived from  
298 the estimation of  $T_{mm}$ . If desired, it is possible to quantify it using probabilistic methods  
299 showed in recent publications.<sup>35,36</sup> Likewise, other sources of uncertainty can arise in  
300 more complex projection scenarios, such as those assuming changes in vulnerability  
301 (adaptation) and population structure. However, these can be more difficult to integrate  
302 quantitatively in the overall estimate of uncertainty.

303

## 304 7. Accounting for complex scenarios: demographic changes and adaptation

305 The example illustrated so far is built under the assumptions of no-adaptation and stable  
306 populations. Findings from this exercise can answer the question: “What will the  
307 temperature-related impact be in the future if the current population would be exposed  
308 to warmer temperatures projected in the future?”. However, there is a growing interest in

309 assessing environmental impacts under more complex scenarios that account for  
310 changes in both future risks and baseline population, which could *a priori* approximate  
311 more realistically future health impacts. This additional section aims at describing these  
312 potential extensions.

313 As mentioned before in the Section 2 of the tutorial, changes in size and population  
314 structure may have a strong influence on future health impacts, both by increasing the  
315 population at risk and by shifting it toward more susceptible groups with higher  
316 associated risks. Some studies have accounted for this using age-specific risks and  
317 outcome rates derived from socio-economic trajectories,<sup>18,19,27,37</sup> defined for example in  
318 the so-called Shared Socio-economic Pathways (SSP).<sup>38</sup> This can be incorporated in this  
319 framework by replicating the proposed procedure by each age category. This step  
320 requires the estimation of age-specific exposure-response associations, as shown in  
321 Figure 6A, and their application over the corresponding future age-specific outcome  
322 series built under a specific SSP. These modelled outcome series can be derived by re-  
323 scaling the observed seasonal counts in the current period using age-specific baseline  
324 populations and rates projected in the future under a specific SSP. However, it should  
325 be noted that, while the “stable populations” approach is built on simplistic assumptions  
326 and cannot provide a realistic representation of future excess burdens, it offers a more  
327 straightforward interpretation as it separates the impact of global warming from other  
328 changes, such as those related to demographic variations, that would occur anyway  
329 even in a stable climate.

330 Another important issue to be considered in health projection studies is the potential  
331 changes in susceptibility to specific environmental stressors. For example, evidence  
332 obtained so far indicates that populations have partly adapted to heat stress in the last  
333 decades, with related risks showing an attenuation along this period.<sup>39</sup> Under these  
334 assumptions, exposure-response associations obtained on historical data would not be  
335 representative of future risks, and several methods have been proposed to address this  
336 issue. These include the analogue city approach,<sup>14,40</sup> which makes use of exposure-  
337 response estimates from a location with a climate similar to that projected in the future,  
338 or methods that allows direct changes in the estimated exposure-response function<sup>41–44</sup>  
339 Both approaches can be incorporated into the proposed framework by replacing or  
340 modifying the estimated exposure-response function. As an illustrative example, Figure  
341 6B shows the modified temperature-mortality curve for London, assuming a decrease in  
342 30% in the mortality log-RR associated with heat only, obtained by applying a scaling  
343 factor to the related part of the curve. However, one should take into account that this  
344 approach, while potentially more realistic, often implies simplistic assumptions on the

345 form of the future exposure-response shape and its changes due to adaptation (e.g.,  
346 linear-threshold shapes, or shifts). In addition, while few studies have used empirical  
347 evidence from historical data,<sup>43</sup> most of them have defined an arbitrary set of parameters  
348 to model the extent and timing of adaptation mechanisms.<sup>42</sup> A recent publication has  
349 discussed problems and limitations of existing methods for modelling adaptation, also  
350 showing how the choice greatly influences the estimated health impacts, and discussing  
351 the difficulties in defining and quantifying valid adaptation mechanisms.<sup>45</sup> Thus, further  
352 implications on the potential limitations of the applied method should be considered and  
353 clearly discussed when assuming hypothetical changes in vulnerability.

354

### 355 **Overview and final remarks**

356 In this contribution, we have presented a well-structured and flexible methodological  
357 framework, based on cutting-edge statistical techniques and clearly defined  
358 assumptions, to obtain health impact projections under climate change scenarios of  
359 variable complexity. Shaped as a hands-on tutorial, this article describes the key  
360 methodological steps through a practical example of an applied analysis, complemented  
361 with real data and R code. While the analytical approaches described in the example are  
362 tailored to the specific study settings, and should not be uncritically applied in a 'cut-and-  
363 paste' approach, this tutorial offers the reader the opportunity to advance through general  
364 methodological steps, following how different statistical choices and assumptions have  
365 been translated in the analysis and code. At the same time, it enables the reader to  
366 replicate, adapt and potentially extend the proposed modelling framework by applying  
367 alternative modelling choices using other environmental stressors, outcomes, study  
368 settings, and more complex climate change scenarios. In a more general context, this  
369 tutorial highlights the need of multi-disciplinary knowledge and skills for projecting health  
370 impacts under climate change scenarios, involving experts working in different research  
371 areas, such as epidemiology, statistics, and climate science, among other subjects. This  
372 contribution clearly advocates for collaborative research and emphasizes the benefits of  
373 reproducibility and transparency in science.

374

375

376

377

378

379 **References**

380

381 1. Petkova EP, Vink JK, Horton RM, et al. Towards More Comprehensive Projections  
382 of Urban Heat-Related Mortality: Estimates for New York City under Multiple  
383 Population, Adaptation, and Climate Scenarios. *Environ Health Perspect.*  
384 2017;125(1):47-55. doi:10.1289/EHP166

385 2. Weinberger KR, Haykin L, Eliot MN, Schwartz JD, Gasparrini A, Wellenius GA.  
386 Projected temperature-related deaths in ten large U.S. metropolitan areas under  
387 different climate change scenarios. *Environ Int.* 2017;107:196-204.  
388 doi:10.1016/j.envint.2017.07.006

389 3. Stowell JD, Kim Y-M, Gao Y, Fu JS, Chang HH, Liu Y. The impact of climate change  
390 and emissions control on future ozone levels: Implications for human health.  
391 *Environ Int.* 2017;108:41-50. doi:10.1016/j.envint.2017.08.001

392 4. Abel DW, Holloway T, Harkey M, et al. Air-quality-related health impacts from  
393 climate change and from adaptation of cooling demand for buildings in the eastern  
394 United States: An interdisciplinary modeling study. *PLoS Med.*  
395 2018;15(7):e1002599. doi:10.1371/journal.pmed.1002599

396 5. Gasparrini A, Guo Y, Sera F, et al. Projections of temperature-related excess  
397 mortality under climate change scenarios. *Lancet Planet Health.* 2017;1(9):e360-  
398 e367. doi:10.1016/S2542-5196(17)30156-0

399 6. Huang C, Barnett AG, Wang X, Vaneckova P, FitzGerald G, Tong S. Projecting  
400 Future Heat-Related Mortality under Climate Change Scenarios: A Systematic  
401 Review. *Environ Health Perspect.* 2011;119(12):1681-1690.  
402 doi:10.1289/ehp.1103456

403 7. Sanderson M, Arbuthnott K, Kovats S, Hajat S, Falloon P. The use of climate  
404 information to estimate future mortality from high ambient temperature: A  
405 systematic literature review. *PLOS ONE.* 2017;12(7):e0180369.  
406 doi:10.1371/journal.pone.0180369

407 8. Kinney PL, O'Neill MS, Bell ML, Schwartz J. Approaches for estimating effects of  
408 climate change on heat-related deaths: challenges and opportunities. *Environ Sci*  
409 *Policy.* 2008;11(1):87-96. doi:10.1016/j.envsci.2007.08.001

410 9. Vicedo-Cabrera AM, Guo Y, Sera F, et al. Temperature-related mortality impacts  
411 under and beyond Paris Agreement climate change scenarios. *Clim Change.*  
412 September 2018. doi:10.1007/s10584-018-2274-3

413 10. Gasparrini A, Guo Y, Hashizume M, et al. Mortality risk attributable to high and low  
414 ambient temperature: a multicountry observational study. *Lancet.* May 2015.  
415 doi:10.1016/S0140-6736(14)62114-0

416 11. Taylor KE, Stouffer RJ, Meehl GA. An Overview of CMIP5 and the Experiment  
417 Design. *Bull Am Meteorol Soc.* 2011;93(4):485-498. doi:10.1175/BAMS-D-11-  
418 00094.1

419 12. Warszawski L, Frieler K, Huber V, Piontek F, Serdeczny O, Schewe J. The Inter-  
420 Sectoral Impact Model Intercomparison Project (ISI-MIP): Project framework. *Proc*  
421 *Natl Acad Sci.* 2014;111(9):3228-3232. doi:10.1073/pnas.1312330110

- 422 13. Kendrovski V, Baccini M, Martinez GS, Wolf T, Paunovic E, Menne B. Quantifying  
423 Projected Heat Mortality Impacts under 21st-Century Warming Conditions for  
424 Selected European Countries. *Int J Environ Res Public Health*. 2017;14(7).  
425 doi:10.3390/ijerph14070729
- 426 14. Knowlton K, Lynn B, Goldberg RA, et al. Projecting Heat-Related Mortality Impacts  
427 Under a Changing Climate in the New York City Region. *Am J Public Health*.  
428 2007;97(11):2028-2034. doi:10.2105/AJPH.2006.102947
- 429 15. Armstrong B. Models for the relationship between ambient temperature and daily  
430 mortality. *Epidemiol Camb Mass*. 2006;17(6):624-631.  
431 doi:10.1097/01.ede.0000239732.50999.8f
- 432 16. Dominici F, Sheppard L, Clyde M. Health Effects of Air Pollution: A Statistical  
433 Review. *Int Stat Rev*. 2003;71:243-276.
- 434 17. Bhaskaran K, Gasparrini A, Hajat S, Smeeth L, Armstrong B. Time series  
435 regression studies in environmental epidemiology. *Int J Epidemiol*.  
436 2013;42(4):1187-1195. doi:10.1093/ije/dyt092
- 437 18. Hajat S, Vardoulakis S, Heaviside C, Eggen B. Climate change effects on human  
438 health: projections of temperature-related mortality for the UK during the 2020s,  
439 2050s and 2080s. *J Epidemiol Community Health*. February 2014.  
440 doi:10.1136/jech-2013-202449
- 441 19. Heaviside C, Tsangari H, Paschalidou A, et al. Heat-related mortality in Cyprus for  
442 current and future climate scenarios. *Sci Total Environ*. 2016;569-570:627-633.  
443 doi:10.1016/j.scitotenv.2016.06.138
- 444 20. Gasparrini A. Modeling exposure-lag-response associations with distributed lag  
445 non-linear models. *Stat Med*. September 2013. doi:10.1002/sim.5963
- 446 21. IPCC. *Climate Change 2007: The Physical Science Basis. Contribution of Working*  
447 *Group I to the Fourth Assessment Report of the Intergovernmental Panel on*  
448 *Climate Change*. Cambridge UK and New York USA: IPCC; 2007.
- 449 22. Moss RH, Edmonds JA, Hibbard KA, et al. The next generation of scenarios for  
450 climate change research and assessment. *Nature*. 2010;463(7282):747.  
451 doi:10.1038/nature08823
- 452 23. Moss RH, Nakicenovic N, O'Neill BC. *Towards New Scenarios for Analysis of*  
453 *Emissions, Climate Change, Impacts, and Response Strategies*. Geneva: IPCC;  
454 2008. [http://www.ipcc.ch/pdf/supporting-material/expert-meeting-report-](http://www.ipcc.ch/pdf/supporting-material/expert-meeting-report-scenarios.pdf)  
455 [scenarios.pdf](http://www.ipcc.ch/pdf/supporting-material/expert-meeting-report-scenarios.pdf). Accessed July 16, 2018.
- 456 24. Baccini M, Kosatsky T, Analitis A, et al. Impact of heat on mortality in 15 European  
457 cities: attributable deaths under different weather scenarios. *J Epidemiol*  
458 *Community Health*. 2011;65(1):64-70. doi:10.1136/jech.2008.085639
- 459 25. Doherty RM, Heal MR, Wilkinson P, et al. Current and future climate- and air  
460 pollution-mediated impacts on human health. *Environ Health*. 2009;8(1):S8.  
461 doi:10.1186/1476-069X-8-S1-S8
- 462 26. Doyon B, Bélanger D, Gosselin P. The potential impact of climate change on annual  
463 and seasonal mortality for three cities in Québec, Canada. *Int J Health Geogr*.  
464 2008;7:23. doi:10.1186/1476-072X-7-23

- 465 27. Ostro B, Barrera-Gómez J, Ballester J, Basagaña X, Sunyer J. The impact of future  
466 summer temperature on public health in Barcelona and Catalonia, Spain. *Int J*  
467 *Biometeorol.* 2012;56(6):1135-1144. doi:10.1007/s00484-012-0529-7
- 468 28. Peng RD, Bobb JF, Tebaldi C, McDaniel L, Bell ML, Dominici F. Toward a  
469 quantitative estimate of future heat wave mortality under global climate change.  
470 *Environ Health Perspect.* 2011;119(5):701-706. doi:10.1289/ehp.1002430
- 471 29. Vardoulakis S, Dear K, Hajat S, Heaviside C, Eggen B, McMichael AJ. Comparative  
472 assessment of the effects of climate change on heat- and cold-related mortality in  
473 the United Kingdom and Australia. *Environ Health Perspect.* 2014;122(12):1285-  
474 1292. doi:10.1289/ehp.1307524
- 475 30. Hewitson BC, Daron J, Crane RG, Zermoglio MF, Jack C. Interrogating empirical-  
476 statistical downscaling. *Clim Change.* 2014;122(4):539-554. doi:10.1007/s10584-  
477 013-1021-z
- 478 31. Maraun D. Bias Correcting Climate Change Simulations - a Critical Review. *Curr*  
479 *Clim Change Rep.* 2016;2(4):211-220. doi:10.1007/s40641-016-0050-x
- 480 32. Hempel S, Frieler K, Warszawski L, Schewe J, Piontek F. A trend-preserving bias  
481 correction – the ISI-MIP approach. *Earth Syst Dynam.* 2013;4(2):219-236.  
482 doi:10.5194/esd-4-219-2013
- 483 33. Wu J, Zhou Y, Gao Y, et al. Estimation and Uncertainty Analysis of Impacts of  
484 Future Heat Waves on Mortality in the Eastern United States. *Environ Health*  
485 *Perspect.* 2014;122(1):10-16. doi:10.1289/ehp.1306670
- 486 34. Gasparrini A, Leone M. Attributable risk from distributed lag models. *BMC Med Res*  
487 *Methodol.* 2014;14:55. doi:10.1186/1471-2288-14-55
- 488 35. Lee W, Kim H, Hwang S, Zanobetti A, Schwartz JD, Chung Y. Monte Carlo  
489 simulation-based estimation for the minimum mortality temperature in temperature-  
490 mortality association study. *BMC Med Res Methodol.* 2017;17(1):137.  
491 doi:10.1186/s12874-017-0412-7
- 492 36. Tobías A, Armstrong B, Gasparrini A. Brief Report: Investigating Uncertainty in the  
493 Minimum Mortality Temperature: Methods and Application to 52 Spanish Cities.  
494 *Epidemiol Camb Mass.* 2017;28(1):72-76. doi:10.1097/EDE.0000000000000567
- 495 37. Jackson JE, Yost MG, Karr C, et al. Public health impacts of climate change in  
496 Washington State: projected mortality risks due to heat events and air pollution.  
497 *Clim Change.* 2010;102(1-2):159-186. doi:10.1007/s10584-010-9852-3
- 498 38. Riahi K, van Vuuren DP, Kriegler E, et al. The Shared Socioeconomic Pathways  
499 and their energy, land use, and greenhouse gas emissions implications: An  
500 overview. *Glob Environ Change.* 2017;42:153-168.  
501 doi:10.1016/j.gloenvcha.2016.05.009
- 502 39. Arbuthnott K, Hajat S, Heaviside C, Vardoulakis S. Changes in population  
503 susceptibility to heat and cold over time: assessing adaptation to climate change.  
504 *Environ Health Glob Access Sci Source.* 2016;15 Suppl 1:33. doi:10.1186/s12940-  
505 016-0102-7

- 506 40. Hayhoe K, Cayan D, Field CB, et al. Emissions pathways, climate change, and  
507 impacts on California. *Proc Natl Acad Sci.* 2004;101(34):12422-12427.  
508 doi:10.1073/pnas.0404500101
- 509 41. Gosling SN, McGregor GR, Lowe JA. Climate change and heat-related mortality in  
510 six cities Part 2: climate model evaluation and projected impacts from changes in  
511 the mean and variability of temperature with climate change. *Int J Biometeorol.*  
512 2009;53(1):31-51. doi:10.1007/s00484-008-0189-9
- 513 42. Huynen MMTE, Martens P. Climate Change Effects on Heat- and Cold-Related  
514 Mortality in the Netherlands: A Scenario-Based Integrated Environmental Health  
515 Impact Assessment. *Int J Environ Res Public Health.* 2015;12(10):13295-13320.  
516 doi:10.3390/ijerph121013295
- 517 43. Honda Y, Kondo M, McGregor G, et al. Heat-related mortality risk model for climate  
518 change impact projection. *Environ Health Prev Med.* 2014;19(1):56-63.  
519 doi:10.1007/s12199-013-0354-6
- 520 44. Dessai S. Heat stress and mortality in Lisbon Part II. An assessment of the potential  
521 impacts of climate change. *Int J Biometeorol.* 2003;48(1):37-44.  
522 doi:10.1007/s00484-003-0180-4
- 523 45. Gosling SN, Hondula DM, Bunker A, et al. Adaptation to Climate Change: A  
524 Comparative Analysis of Modeling Methods for Heat-Related Mortality. *Environ*  
525 *Health Perspect.* 2017;125(8):087008. doi:10.1289/EHP634

526  
527

528

529

530

531

532

533

534

535

536

537

538

539

540

541

542



543 **Figure legends**

544 **Figure 1. Temperature-related mortality in London (1990-2012).** Left panel: three-  
545 dimensional plot showing the estimated exposure-lag-response association between  
546 temperature and mortality. Mid panel: overall cumulative mortality risk (and 95%  
547 confidence interval). Right panel: comparison between the exposure-response shapes  
548 estimated using three modelling approaches.

549 **Figure 2. Temporal trends in projected temperature in London (1971 - 2099).** Solid  
550 lines correspond to the mean annual temperature estimated across the 5 GCMs-specific  
551 modelled series. The shaded area shows its variability, corresponding to the range for  
552 each year. The two horizontal bars in the right correspond to the average annual  
553 maximum and minimum for each modelled temperature series.

554 **Figure 3. Seasonal mortality trends in London.** Grey dots correspond to the observed  
555 daily mortality counts registered in each day of the year between 1990 and 2012. The  
556 blue line depicts the mean number of deaths per day of the year.

557 **Figure 4. Bias-correction of the modelled temperature series.** Comparison between  
558 the distribution (left panel) and cumulative distribution (right panel) of the raw and bias-  
559 corrected modelled temperature ( $T_{mod}$ ,  $T_{mod}^*$ ), and the observed temperature series  
560 ( $T_{obs}$ ).

561 **Figure 5. Temperature and excess mortality in London for present and future**  
562 **periods.** Top panel: exposure-response curve represented as mortality relative risk (RR)  
563 across the temperature ( $^{\circ}\text{C}$ ) range, with 95% empirical confidence intervals (grey area).  
564 The dotted vertical line corresponds to the minimum mortality temperature ( $T_{mm}$ ) used  
565 as reference, which defines the two portions of the curve related to cold and heat (blue  
566 and red, respectively). The dashed part of the curve represents the extrapolation beyond  
567 the maximum temperature observed in 2010-19 (dashed vertical line). Mid panel:  
568 distribution of  $T_{mod}^*$  for the current (2010-19, grey area) and at the end of the century  
569 (2090-99, green area), projected using a specific climate model (NorESM1-M) and  
570 scenario (RCP8.5). Bottom panel: the related distribution of excess mortality, expressed  
571 as the fraction of additional deaths (%) attributed to non-optimal temperature compared  
572 with  $T_{mm}$ .

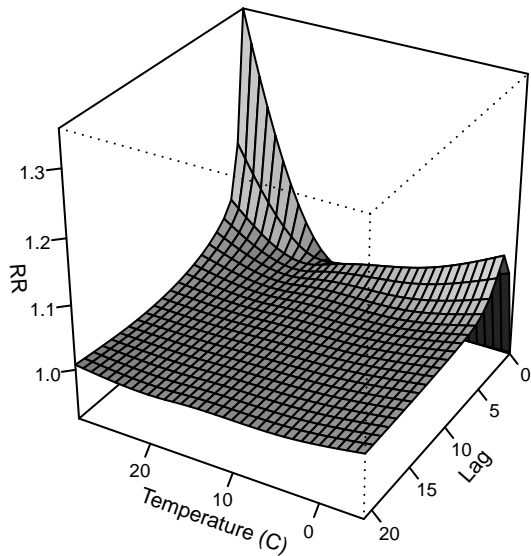
573 **Figure 6. Accounting for complex scenarios accounting for socio-demographic**  
574 **changes and adaptation.** Right panel: age-specific exposure-response curves,  
575 applicable to project health impact separately for each age category, thus potentially  
576 accounting for demographic changes by using differential baseline mortality trends. Left  
577 panel: comparison between the exposure-response curves under scenarios of no

578 adaptation (continuous line) and adaptation (dashed line), the latter under the (simplistic)  
579 assumption of an hypothetical attenuation of 30% in risk associated to heat.

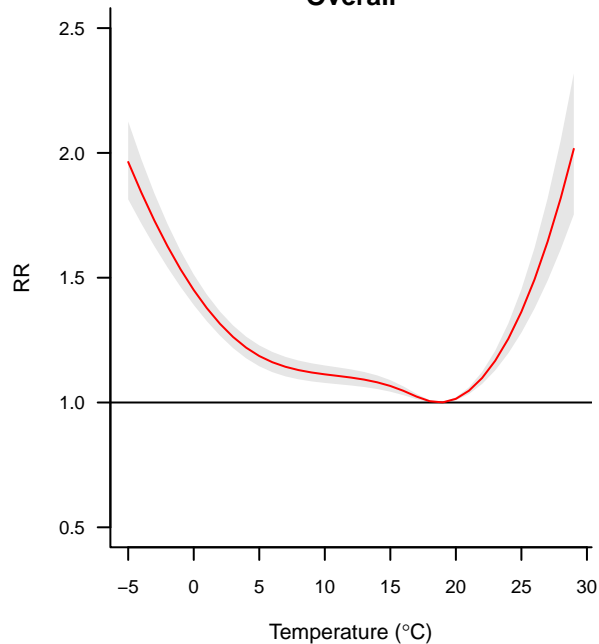
# London

1990–2012

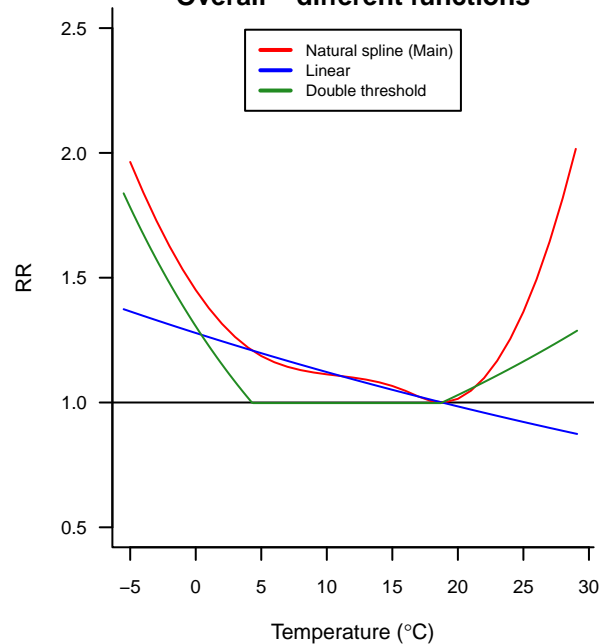
### Exposure-lag-response



### Overall

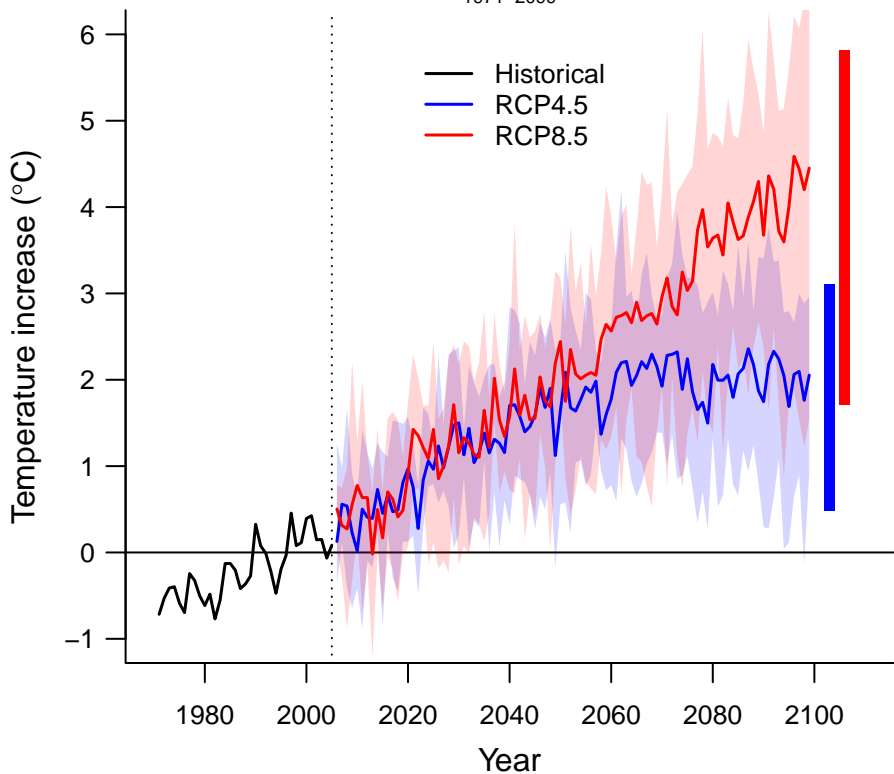


### Overall – different functions



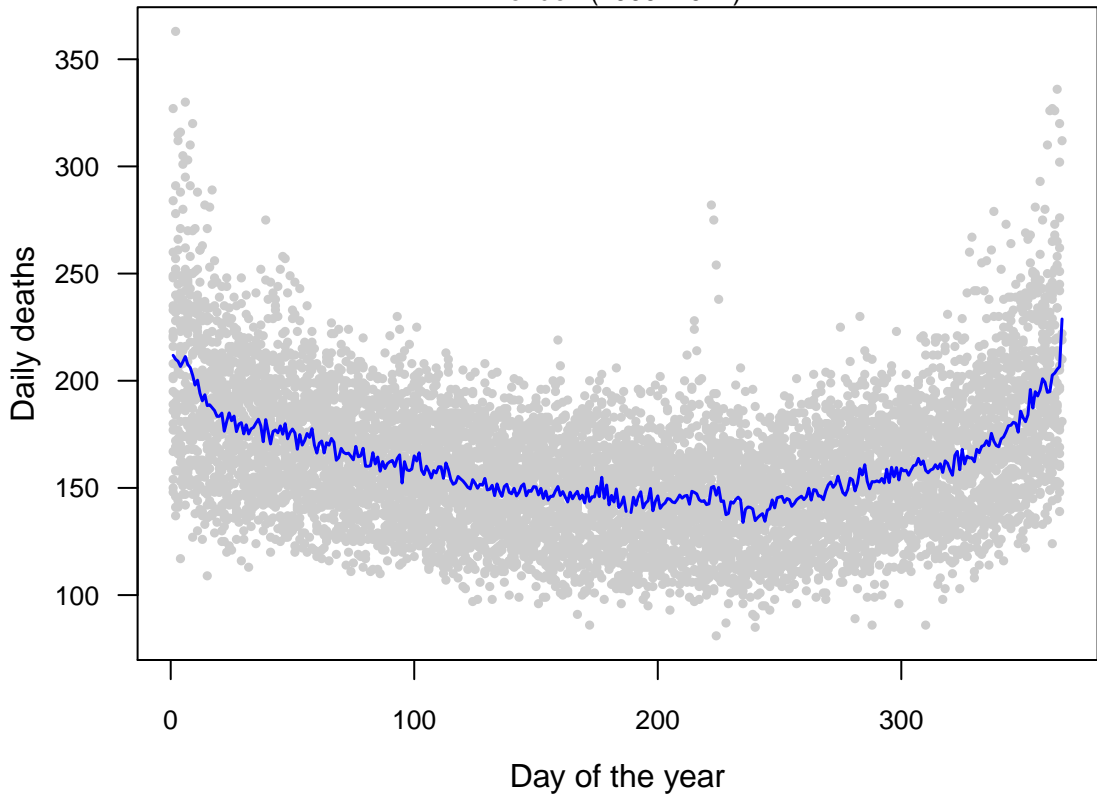
# London

1971–2099



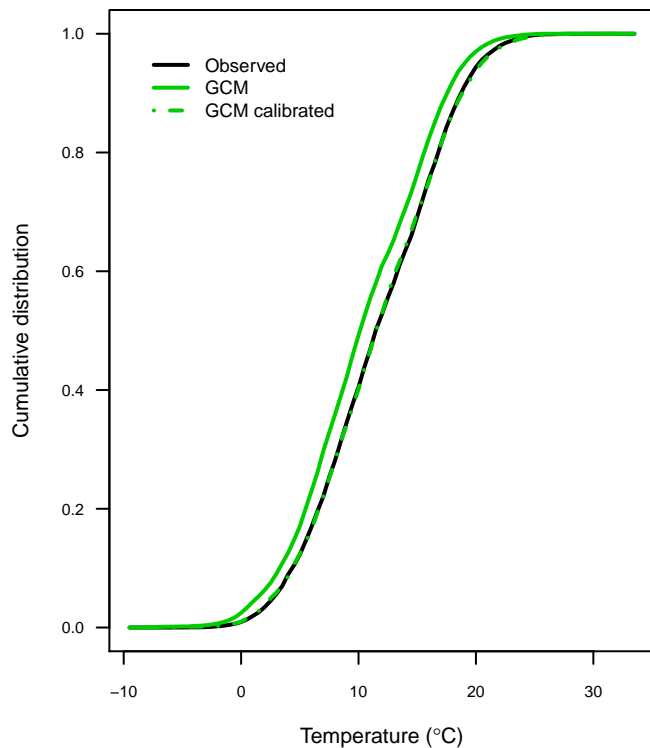
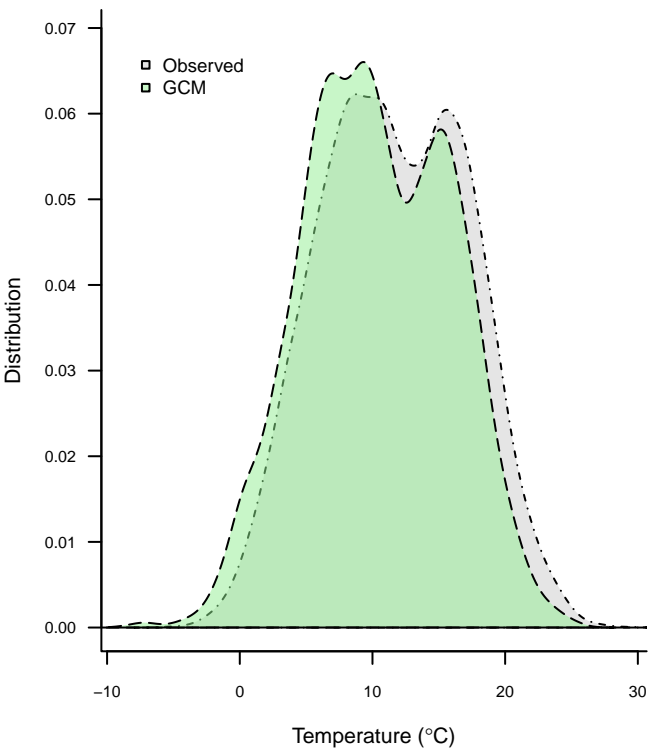
# Observed Mortality

London (1990–2012)



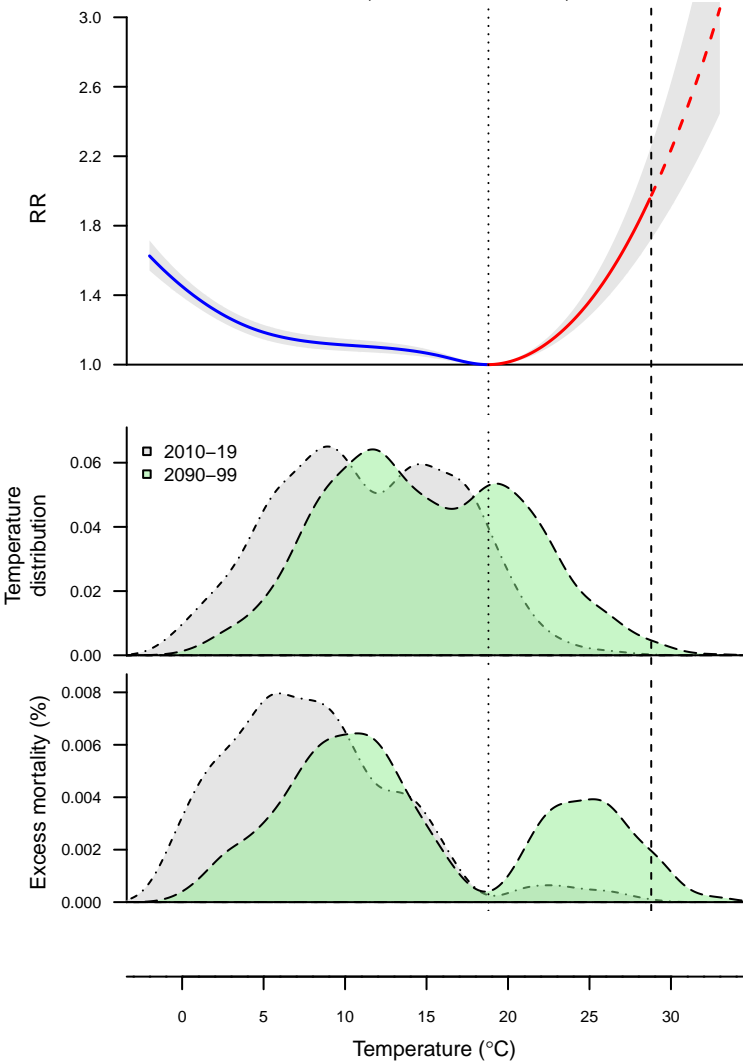
# Calibration

London (1990–2012)

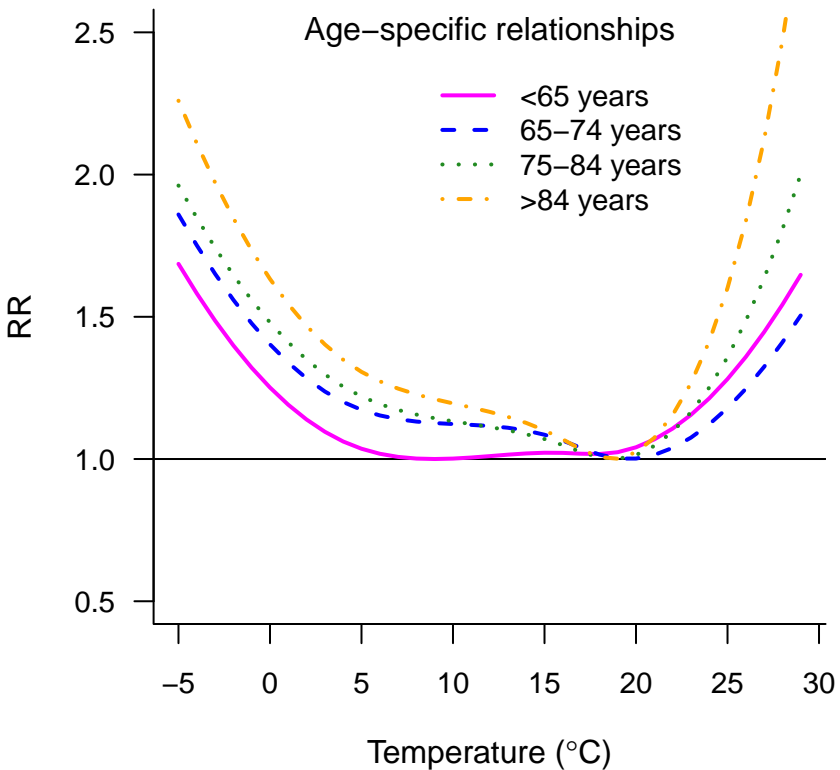


# Temperature-related mortality impacts

London (NorESM1-M – RCP8.5)



## Demographic changes



## Adaptation

